

Radiochemical separation of ^{26}Al and ^{41}Ca from proton-irradiated vanadium targets for cross-section determination by means of AMS

Journal Article

Author(s):

Veicht, Mario; Mihalcea, Ionut; Gautschi, Philip; Vockenhuber, Christof; Maxeiner, Sascha; David, Jean-Christophe; Chen, Shaohuang; Schumann, Dorothea

Publication date:

2022-10

Permanent link:

<https://doi.org/https://doi.org/10.3929/ethz-b-000576144>

Rights / license:

[Creative Commons Attribution 4.0 International](#)

Originally published in:

Radiochimica Acta 110(10), <https://doi.org/10.1515/ract-2022-0036>

Funding acknowledgement:

- Towards implementing new isotopes for environmental research: The half-life of ^{32}Si ()



Mario Veicht, Ionut Mihalcea*, Philip Gautschi, Christof Vockenhuber, Sascha Maxeiner, Jean-Christophe David, Shaohuang Chen and Dorothea Schumann

Radiochemical separation of ^{26}Al and ^{41}Ca from proton-irradiated vanadium targets for cross-section determination by means of AMS

<https://doi.org/10.1515/ract-2022-0036>

Received March 16, 2022; accepted June 8, 2022;

published online June 22, 2022

Abstract: This work exhibits the very first experimentally determined cross sections for ^{26}Al and ^{41}Ca as proton-induced spallation products of metallic vanadium targets. Additionally, the authors describe a radiochemical separation of ^{26}Al and ^{41}Ca from the vanadium matrix and present the theoretically calculated cross-section values as a reference for the experimental ones.

Keywords: Al-26; Ca-41; cross-section determination; radiochemical separation.

1 Introduction

Nuclear data, such as cross sections for particular reactions are of high interest for filling the gaps in the nuclear databases. Such data are important for various applications, from radiation dose rate estimation in the future subcritical reactors Accelerator-Driven Systems (ADS) to exotic nuclide production yield estimation. Structural components and shielding used in the construction of ADS will be subjected to intense, long-term

particle irradiation. Depending on their composition, various radioactive isotopes are generated and contribute to the induced radiation dose rate. Knowledge of the $^{51}\text{V}(p,x)$ reactions cross-sections helps estimate this dose rate regarding the potential vanadium content in the structure materials. Same data are needed for estimating the production yield and overall cost of radionuclides for particular applications. Rare radionuclides such as ^{26}Al and ^{41}Ca are of high interest in medical, astrophysical, and environmental scientific investigations and applications.

In the past seven decades, the proton-induced reactions on vanadium targets were described in over two dozen scientific reports and the production cross-sections of 55 nuclides at various incident proton beam energies were reported [1]. However, the production cross-sections of ^{26}Al and ^{41}Ca were never reported. The very first experimental cross-section determination for spallation products of vanadium targets was reported by Rudstam in 1953 [2] and ever since an increasing number of specific spallation products have been investigated. Likely, due to difficulties in accurately determining the produced number of atoms or activity for ^{26}Al and ^{41}Ca , their production cross-sections and implicitly the excitation function through vanadium spallation were not determined.

Due to their decay mode and relatively long half-lives, both ^{26}Al ($T_{1/2} = 7.17(24) \cdot 10^5$ y [3]) and ^{41}Ca ($T_{1/2} = 9.94(15) \cdot 10^4$ y [4]) require high sensitivity measurement methods to accurately quantify them as spallation products, especially when the produced amounts are low.

The most accurate way of determining small amounts of long-lived radionuclides is utilizing accelerator mass spectrometry (AMS). Before such measurements, a radiochemical separation is required, followed by careful sample preparation, to provide pure and suitable samples. During the years, AMS has been recognized and established as a leading technique for the determination of long-lived radionuclides [5–9]. In the specific cases of ^{26}Al and ^{41}Ca , the first measurements were performed in 1979 [10] and 1984 [11], respectively.

Data as presented in this paper do not only fill gaps in the nuclear databases but also help to improve the

*Corresponding author: Ionut Mihalcea, Laboratory of Radiochemistry, Paul Scherrer Institut (PSI), Forschungsstrasse 111, CH-5232 Villigen, Switzerland, E-mail: ionut.mihalcea@psi.ch

Mario Veicht, Laboratory of Radiochemistry, Paul Scherrer Institut (PSI), Forschungsstrasse 111, CH-5232 Villigen, Switzerland; and École Polytechnique Fédérale de Lausanne (EPFL), Route Cantonale, CH-1015 Lausanne, Switzerland

Philip Gautschi and Christof Vockenhuber, Laboratory of Ion Beam Physics, Swiss Federal Institute of Technology, Otto Stern Weg 5, CH-8093 Zurich, Switzerland

Sascha Maxeiner, IonPlus AG, CH-8953 Dietikon, Switzerland

Jean-Christophe David, IRFU, CEA, Université Paris-Saclay, F-91191 Gif-sur-Yvette, France

Shaohuang Chen, Department of Chemistry, Simon Fraser University (SFU), Burnaby, BC V5A 1S6, Canada

Dorothea Schumann, Laboratory of Radiochemistry, Paul Scherrer Institut (PSI), Forschungsstrasse 111, CH-5232 Villigen, Switzerland

theoretical models. Therefore, a comparison with experimentally obtained data highlights, whether predictions based on the theoretical models are over- or under-estimating the actual production of radionuclides through various nuclear reactions. Here, excitation functions for ^{26}Al and ^{41}Ca were calculated using Liège Intranuclear Cascade (INCL)/ABLA.

2 Experimental studies

All chemicals used in this work were of p.a. quality or better. Peristaltic pumps (REGLO Digital MS-2/8, Cole-Parmer Instrument Company, LLC., USA) were used for the separations, combined with Ismaprene PharMed[®] (Cole-Parmer Instrument Company, LLC., USA) squeeze tubes. The method development focused first on cold, non-active model solution matching precisely the chemical composition of the active matrix. The inactive experiments were also used to optimize the separation conditions, including the required amount of resin, eluent volumes, and flow rates for the different stages of the separation. The reader is made aware, that ^{32}Si was also separated from the matrix, but not mentioned in the results and discussion, since a suitable AMS-Standard is presently (at the time of submission) not available.

2.1 Pretreatment of the irradiated targets

Vanadium metallic discs with a diameter of 15 mm and thickness of 1 mm were used as targets. Notably, the irradiation of these specimen took place between October 1995 and March 1996. The initial target preparation was performed in joint cooperation of the University of Cologne and the Leibnitz University Hannover. The targets are therefore originating from the extensive irradiation experiments, performed by Michel and colleagues (e.g., [12]). Furthermore, information concerning the irradiation conditions and the detailed chemical processing have been reported elsewhere [13], but are also provided (see the Supplementary Table 2).

In the initial treatment, the seven proton-irradiated targets were each solubilized, resulting in solutions with a volume of 5 mL. Each solution contained the full chemical matrix of the target material, dissolved in 8 M HCl.

2.2 Matrix change and silicon removal

Each ion-exchange or extraction column chromatography employed in this work generally comprises three stages:

the loading phase, in which the stationary phase is put in contact with the solution to be separated; the washing phase, employed for the complete removal of the non-binding elements; and the eluting phase, for recovering the binding elements.

Since the samples were intended for AMS measurements, carriers for both calcium and aluminum had to be added before the separation. Therefore, 2 mL of each single-element standard solution (1000 mg/L, Trace-CERT[®], Merck KGaA, Germany) was added. Additionally, 2 mL of a freshly prepared 1 M L-ascorbic acid (Merck KGaA, Germany) was added, before being further diluted to a final volume of 200 mL with ultra-pure water (18.2 M Ω , Veolia S.A., France).

In the first separation, Dowex[®] 50WX8-200 (Merck KGaA, Germany) is used, a strong-acidic cation exchange resin as stationary phase, hosted in a tailor-made polymethyl methacrylate (PMMA) column with an inner diameter of 10 mm and the resin bed height of 140 mm. The loading phase consisting of 200 mL full matrix solution was followed by a washing phase of 30 mL H₂O, and the two fractions were collected together. The eluting phase consisted of 50 mL 3 M HNO₃, and was collected separately.

For the method development part, a model solution was prepared by dissolving a vanadium disc weighing 0.4125 g in 5 mL 8 M HNO₃. The obtained solution was transferred in a 10 mL volumetric flask and brought to quota with H₂O. From the resulted solution a volume of 3.2 mL was transferred on a PTFE evaporation dish (6 cm diameter, 1 cm height) and evaporated to dryness, followed by decomposition to oxide (approx. 250°C). The resulting solid oxide residue was further dissolved in 5 mL 8 M HCl solution and quantitatively transferred to a 200 mL volumetric flask. Standard 1000 ppm solutions of Si, Ca, and Al, 2 mL each, were successively added, followed by 3 mL of 0.5 M N₂H₄. Lastly, the solution was brought to the quota with H₂O.

The resulting solution (200 mL) was loaded on a chromatographic column containing AG[®]-50W-X8 cation exchange resin (140 mm resin bed height, 9 mm diameter). The loading eluate was collected in four fractions of 50 mL each, and their content was analyzed via Inductively Coupled Plasma-Optical Emission Spectrometry (ICP-OES) without further dilution. The washing step, consisting of 30 mL H₂O was collected in three fractions of 10 mL each and similarly analyzed. Finally, the eluting phase, consisting of 50 mL 3 M HNO₃ was collected in five individual fractions, each diluted 10-fold before being analyzed. The elements concentrations were measured via ICP-OES against a five-point calibration curve with a maximum standard concentration of 20 ppm for Al and Ca, 10 ppm for

Si, and 400 ppm for V. The selected measurement wavelengths were 396.152 nm for Al, 396.847 nm for Ca, 251.611 nm for Si, and 326.769 nm for V.

2.3 ^{41}Ca separation

It has been reported [14] that ^{41}Ca shows high retention in 3 M HNO_3 onto DGA resin (TrisKem International SAS, France) so the elute phase was specifically chosen for the consecutive separation of ^{41}Ca from the matrix. Each solution yielded 50 mL acidic solution, which was then loaded onto the DGA resin. Again, a tailor-made PMMA column (length = 100 mm; inner diameter = 10 mm) was chosen to host the resin. After the load solution passed through, 20 mL of 3 M HNO_3 was employed as wash phase, yielding a total volume of 70 mL. Finally, ^{41}Ca was collected in 30 mL of 3 M HCl.

The method development consisted of the preparation of a 50 mL solution containing Al and Ca, 2 mg each, and V, 132 mg, with a HNO_3 concentration of 3 M. Next, the solution was loaded onto a chromatographic column containing DGA resin (45 mm resin bed height, 9 mm diameter). The load eluate was collected in five fractions of 10 mL each, 10-fold diluted, and the concentration of the elements of interest was measured via ICP-OES. The wash and elute solutions were each collected in three 10 mL fractions and analyzed similarly. The concentrations for the elements of interest were measured using ICP-OES, similar was the case of silicon removal, against a five-point calibration curve, but with maximum standard concentrations ranging up to 10 ppm for Al, 20 ppm for Ca, and 300 ppm for V. The selected measurement wavelengths were 396.152 nm for Al, 396.847 nm for Ca, and 292.401 nm for V.

2.4 ^{26}Al separation

In the case of ^{26}Al , we chose a gradual elution from the vanadium matrix. Upon the addition of 7 mL H_2O_2 (30% w/w, Merck KGaA, Germany) to the previous 70 mL solution (3 M HNO_3), the solution turned red, indicating the presence of the oxo-peroxo $[\text{VO}(\text{O}_2)]^+$ cationic complex. Consequently, the solution was heated up for 10 min in a water bath (keeping at $\approx 60^\circ\text{C}$) and immediately placed in ice, to stop the gradual decomposition of the hydrogen peroxide, and thus the oxo-peroxo vanadium complex. To decrease the acidity for the initial separation, the solution was then diluted to 310 mL using a graduated cylinder, resulting in ≈ 0.75 M HNO_3 . Again, Dowex[®] 50WX8-200

was used (bed height: 140 mm), filled in the tailor-made 300 mm PMMA-column. The separation scheme then included a wash with 30 mL 0.75 M HNO_3 , followed by 10 mL 1 M HNO_3 , and 20 mL 3 M HNO_3 . Those volumes were collected in a single PE bottle and subsequently disposed of, as it contained only vanadium. Ultimately, the elute phase consisted of 30 mL 3 M HNO_3 and was collected separately.

In the development stage, a 340 mL solution containing 2 mg Al, 132 mg V, and 7 mL H_2O_2 30% (w/w) with a HNO_3 concentration of approximately 0.75 M was prepared and loaded onto a chromatographic column containing Dowex[®] 50WX8-200 resin (140 mm resin bed height, 9 mm diameter). The load eluate was collected in a single fraction of 340 mL, one hundredfold diluted and the concentrations of the elements of interest were measured via ICP-OES. The two wash and the elute solutions were each collected in 5 mL fractions, 10-fold diluted, and analyzed similarly. The concentrations for the elements of interest were also measured using ICP-OES against a five-point calibration curve with a maximum standard concentration of 20 ppm for both Al and V. The selected measurement wavelengths were 396.152 nm for Al and 292.401 nm for V.

The developed separation methods were applied to the irradiated targets solutions described above, to obtain the final sample material for AMS measurements.

2.5 AMS sample preparation and measurements

Each ^{41}Ca -fraction was evaporated to dryness using a 5 mL conical glass vial while successively adding the acidic solution. The heat was applied by an external electric heating coil with the temperature set to 150°C . The obtained solid residues were dissolved in 0.5 mL H_2O and the resulting solutions were transferred to a 2 mL centrifuge plastic vial. Moreover, 0.25 mL 1 M HF was added to account for the stoichiometry, and the solutions were left undisturbed overnight for CaF_2 precipitation. The dispersion was then centrifuged and the supernatant was discarded. The solid precipitate was dispersed in 0.75 mL H_2O and the centrifugation process was once again repeated. The obtained solids were dried for 24 h at 80°C before being sent to the AMS facility. The AMS measurement was performed at the 300 kV MILEA AMS [15] following the procedure described by Vockenhuber et al. [16]. At the low energies available at MILEA the isobars cannot be clearly separated as with the gas ionization detector but the intensity of K can be significantly reduced by selecting

CaF_3^- . Furthermore, the contribution of ^{41}K to the mass 41 counts can be monitored by measuring the isotope ^{39}K and a correction can be applied assuming a constant (natural) $^{41}\text{K}/^{39}\text{K}$ ratio. Standards B10 and B9 were used for normalization with nominal values taken from Ref. [5]. A blank correction based on the average of three blanks was applied and an uncertainty of 3% was added to the relative uncertainty.

For the separated ^{26}Al solutions, the initial sample volume of 30 mL was reduced to 5 mL by evaporation. The concentrated solutions were then transferred to a 50 mL conical centrifugation vessel.

For each, the pH was adjusted to 9.6 (3) with the addition of half-concentrated ammonia (NH_3) solution. The resulting precipitate was allowed to settle overnight, the solution was centrifuged, the supernatant was discarded and the solids were dried at 105°C in a glazed crucible for 24 h. Once dried, the solids were calcined at 900°C for 12 h before being sent for AMS analysis. The ^{26}Al AMS measurement was performed at the 300 kV MILEA AMS facility [15]. Usually, ^{26}Al is measured in charge state 2+ for high transmission and efficiency, but it requires a gas absorber cell in front of the final detector to stop the m/q interference of $^{13}\text{C}^+$. However, the samples here showed too much ^{13}C and, thus, the 1+ charge state was selected, although with a lower transmission. Molecular interferences were sufficiently reduced by increasing the stripper gas pressure. The measured $^{26}\text{Al}/^{27}\text{Al}$ ratios of the irradiated samples were between 1×10^{-12} and 1×10^{-11} whereas the blanks were at 1×10^{-14} and thus not relevant. The measurement was normalized to the internal standard ZAL02 with a nominal $^{26}\text{Al}/^{27}\text{Al}$ ratio of $(46.4 \pm 0.1) \times 10^{-12}$, which, in turn, was calibrated against the primary standard KN 01-4-1 (nominal $^{26}\text{Al}/^{27}\text{Al}$ ratio $[74.44 \pm 2.68] \times 10^{-12}$). A 1% uncertainty was added to the final error.

3 Cross-section determination

3.1 Theoretical cross-section calculations

The theoretical calculations predicting cross-section values for the $^{\text{nat}}\text{V}(p,x)^{26}\text{Al}$, ^{41}Ca reactions, were performed using the Liège Intranuclear Cascade model INCL++ [17, 18] combined with the de-excitation codes ABLA07 [19]. This model combination is usually chosen to compute the production yields and characteristic particles and nuclei generated in spallation reactions [20]. The progenitors were taken into consideration to calculate the cumulative cross-sections using:

$$\sigma_{\text{D,cml}} = \sigma_{\text{D,ind}} + \sigma_{\text{M,cml}} \frac{\lambda_{\text{M}}}{\lambda_{\text{M}} - \lambda_{\text{D}}} \quad (1)$$

Here $\sigma_{\text{D,cml}}$ is the cumulative and $\sigma_{\text{D,ind}}$ is the independent cross-section, $\sigma_{\text{M,cml}}$ is the cross-section of the parent nuclide, λ_{M} is the decay constant of the mother, and λ_{D} is the decay constant of the daughter. $\sigma_{\text{M,cml}}$ is calculated like $\sigma_{\text{D,cml}}$ making the latter a sum of possibly numerous terms, according to the number of successive progenitors. The details can be found elsewhere [19–21].

3.2 Experimental cross-section determination

The AMS measurements provide isotopic ratios between the artificially produced nuclide and a naturally abundant one, present as the carrier. For our experiments, the determined ratios were $^{26}\text{Al}/^{27}\text{Al}$ and $^{41}\text{Ca}/^{40}\text{Ca}$. The total activity for the two nuclides was calculated using:

$$A_{^{26}\text{Al}} = ^{26}\text{Al}/^{27}\text{Al} \cdot N_{^{27}\text{Al}} \cdot \lambda_{^{26}\text{Al}} \quad (2)$$

$$A_{^{41}\text{Ca}} = ^{41}\text{Ca}/^{40}\text{Ca} \cdot N_{^{40}\text{Ca}} \cdot \lambda_{^{41}\text{Ca}} \quad (3)$$

The activity is further used to obtain the specific nuclide production cross-section using Eq. (4), where N_{T} = number of target atoms (here: vanadium), t_{w} = decay period after irradiation, and t_{irr} = irradiation duration. More details are presented in Supplementary Table 2.

$$\sigma = \frac{A \cdot e^{\lambda t_{\text{w}}}}{N_{\text{T}} \cdot \Phi_p (1 - e^{-\lambda t_{\text{irr}}})} \quad (4)$$

All presented uncertainties are quoted with a coverage factor $k = 1$, i.e., confidence level of about 68%.

4 Results and discussion

4.1 Matrix change and silicon removal

The initial separation procedure, employing Dowex[®] 50WX8-200 ion-exchange resin, was required to change the chemical matrix content from 8 M HCl to 3 M HNO_3 . This step also has the added benefit of removing neutral and anionic impurities from the initial matrix, but also silicon-32 that was already identified as a spallation product of proton-irradiated vanadium targets [22].

To begin with, the initial acidic solution was diluted to approximately 0.2 M HCl. Under these conditions, the resin retained most of the cationic species from the solution,

including Ca^{2+} and Al^{3+} cations. During the wash phase, the remnant neutral and anionic species (here: Cl^-) were removed from the column. Finally, 3 M HNO_3 is used for elution.

Before applying the method to the irradiated samples, test experiments were performed with inactive materials, to study the element's behavior under different conditions. The elution profile is represented in Figure 1 and it shows a good separation of V, Al, and Ca from the non-cationic species.

4.2 ^{41}Ca separation

Using 3 M HNO_3 media, DGA shows high selectivity toward Ca^{2+} while letting the other matrix components pass through. The 3 M HCl solution was chosen as eluent since it was previously reported [14] to remove Ca^{2+} from DGA. The model experiment shows an elution profile (see, Figure 2) which confirms that in HNO_3 media there is no retention of Al^{3+} and $\text{V}^{+4/+5}$ by the DGA resin. At the same time Ca^{2+} is fully retained and is eluted in the last step using the HCl media.

4.3 ^{26}Al separation

This step relies on the low affinity of VO_2^+ toward cation exchange resins. However, upon the addition of hydrogen peroxide (H_2O_2), the formation of the red oxo-peroxo $\text{VO}(\text{O}_2)^+$ species was visible, which was found to have a fairly low affinity, too. After adding H_2O_2 , the solution was heated up to promote the decomposition of H_2O_2 excess. To stabilize the $\text{VO}(\text{O}_2)^+$ species, the solution was then placed into an ice bath before the separation started. Employing this procedure, on average ($n=3$) $3.6 \pm 0.3\%$ ($\approx 475.2 \pm 1.4 \mu\text{g}$) of the vanadium was still found when using elevated HNO_3 concentrations,

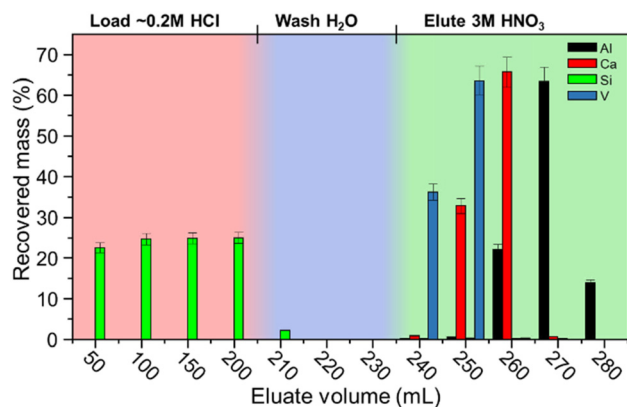


Figure 1: Elution profile for elements of interest on Dowex® 50WX8-200 strong cation exchange resin.

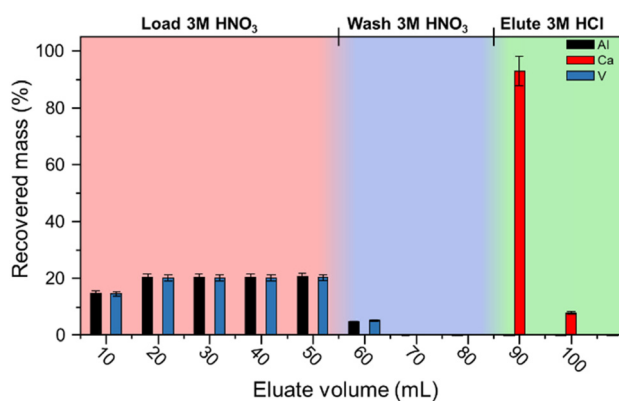


Figure 2: Elution profile for elements of interest on DGA extraction resin.

indicating the presence of V^{+IV} , which has a higher affinity than V^{+V} . To quantitatively remove vanadium, three different HNO_3 concentrations (0.75, 1, and 3 M) were used, following the concept of gradual elution. Therefore, V^{+V} species were removed first, followed by V^{+IV} that exhibits a higher affinity toward the ion-exchange resin. When using 3 M HNO_3 as eluent, both V^{+IV} and Al^{3+} are eluted, so care was taken to obtain pure Al^{3+} -fractions.

For the model experiment, vanadium is oxidized to V^{+V} to lower the affinity for the cation exchange resin but the results show a partial reduction back to V^{+IV} . The elution profile shows over 96% of vanadium being oxidized and passing through the column unretained. The rest is V^{+IV} and is recovered in the two successive wash steps. The first wash step is to ensure the complete elution of V^{+V} while the second is applied to elute the V^{+IV} . In the elute step, the Al is quantitatively recovered. An example of an elution profile, applying the optimized conditions, is provided (see Figure 3).

The entire stepwise separation scheme is depicted in Figure 4.

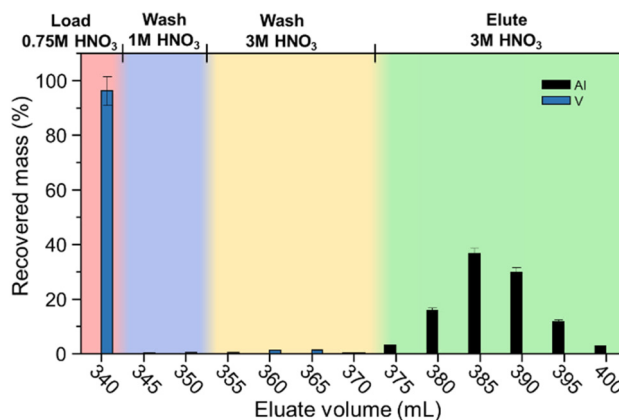


Figure 3: Elution profile for V and Al on Dowex® 50WX8-200 strong cation exchange resin.

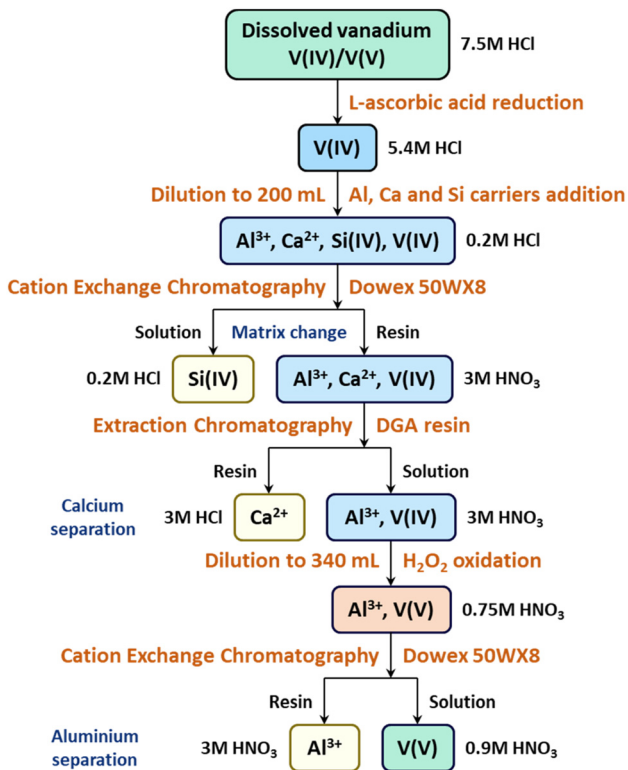


Figure 4: Separation of ^{26}Al and ^{41}Ca from vanadium matrix.

4.4 AMS samples characteristics

The final chemical form for the ^{26}Al and ^{41}Ca samples was chosen to be Al_2O_3 and CaF_2 , respectively, since AMS measurements are already developed for these types of materials [7, 9]. The summed-up separation and

sample preparation yield was on average 67% for Al samples and 94% for the Ca ones (see the Supplementary Table 1).

4.5 Cross-section determination

Comparing the predicted excitation function with the experimental values, for the production of ^{26}Al , the theoretical models seem to slightly underestimate the cross-sections values at low proton energy (<200 MeV) and to overestimate it at higher energy. Nevertheless, the experimental data confirm the predicted low reaction probability for ^{26}Al production by vanadium spallation at incident proton energy below 200 MeV. For the case of ^{41}Ca production, the experimental values show a very good fit to the predicted theoretical model, confirming both the accuracy of the experimental method as well as the predictive power of the theoretical model. A graphical representation of the two excitation functions, showing both the experimental and the predicted cross-sections values, is shown in Figure 5. Calculation details for the experimentally obtained cross-section values are presented in Supplementary Tables 3 and 4. The uncertainty associated with the cross-section values averages at 6.4% for the ^{26}Al samples, with significant contributions coming from the decay constant ($\lambda_{\text{Al-26}}$) and the AMS measurement, weighing on average 28% and 59%, respectively, to the final uncertainty budget. In the case of ^{41}Ca samples, the total uncertainty averages at 4.9%, with major relative contributions from the AMS measurement, the irradiation proton flux, and $\lambda_{\text{Ca-41}}$, weighing on average 66%, 13%, and

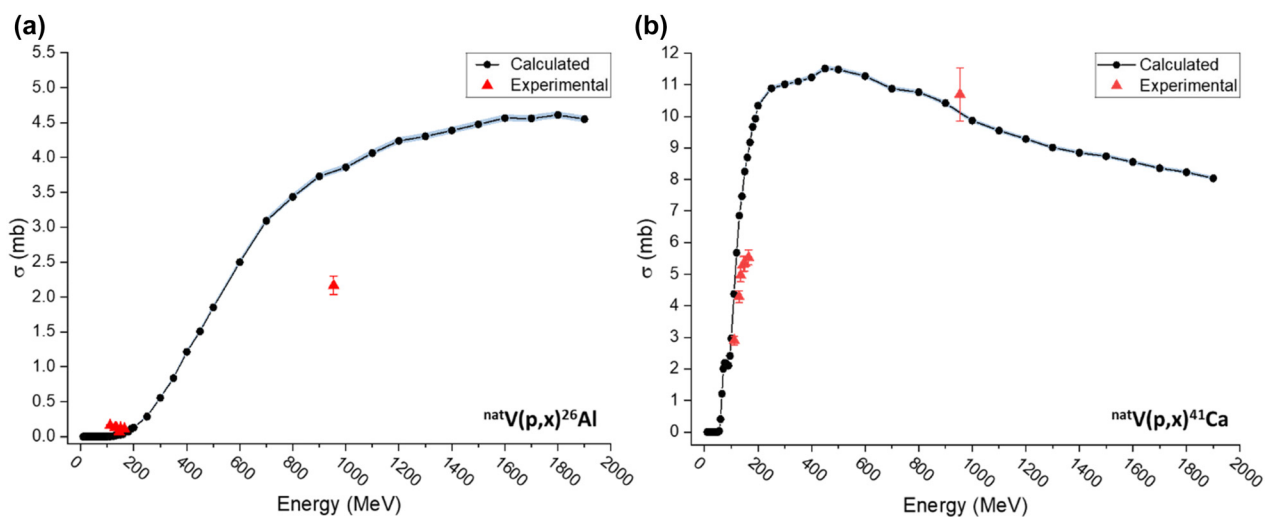


Figure 5: Calculated and experimentally obtained excitation functions, for the nuclear reactions $^{\text{nat}}\text{V}(p,x)^{26}\text{Al}$ (a) and $^{\text{nat}}\text{V}(p,x)^{41}\text{Ca}$ (b).

respectively 11%. A more detailed analysis of individual relative uncertainty values and their contribution to the final budget is shown in Supplementary Tables 5 and 6.

5 Conclusions

Seven vanadium targets were irradiated with protons at energies up to 954 MeV. Following the radiochemical separation, the number of produced ^{26}Al and ^{41}Ca atoms was determined using AMS. To the authors' best knowledge, the production cross-sections for the nuclear reactions of $^{nat}\text{V}(p,x)^{26}\text{Al}$, and $^{nat}\text{V}(p,x)^{41}\text{Ca}$, are reported here for the first time. Generally, an excellent agreement between the calculated and experiment-based excitation function can be observed for ^{41}Ca . However, somewhat scattered values for the cross-sections were obtained for ^{26}Al , leading to a different trend in the presented excitation function, compared to the theoretical predictions.

Acknowledgments: We thank R. Michel and E. Strub for providing the irradiated samples from the target collection of the division of nuclear chemistry at the University of Cologne.

Author contributions: All the authors have accepted responsibility for the entire content of this submitted manuscript and approved submission.

Research funding: This project is funded by the Swiss National Science Foundation (SNSF) as part of SINERGIA (No. 177229) and receives additional financial support from the European Union Horizon 2020 program under Marie Skłodowska-Curie grant agreement No. 701647.

Conflict of interest statement: The authors declare no conflicts of interest regarding this article.

References

- Zerkin V. *Experimental Nuclear Reaction Data (EXFOR)*; International Atomic Energy Agency (IAEA): Vienna, Austria, 2022.
- Rudstam S. G. CXIX. Spallation of vanadium, manganese, and cobalt with 187 MeV protons. *Lond. Edinb. Dublin Philos. Mag. J. Sci.* 1953, 44, 1131–1141.
- Basunia M. S., Hurst A. M. Nuclear data sheets for $A = 26$. *Nucl. Data Sheets* 2016, 134, 1–148.
- Nesaraja C. D., McCutchan E. A. Nuclear data sheets for $A = 41$. *Nucl. Data Sheets* 2016, 133, 1–220.
- Christl M., Vockenhuber C., Kubik P. W., Wacker L., Lachner J., Alfimov V., Synal H. A. The ETH Zurich AMS facilities: performance parameters and reference materials. *Nucl. Instrum. Methods Phys. Res. B.* 2013, 294, 29–38.
- Fenclova K., Prasek T., Nemeš M., Christl M., Gautschi P., Vockenhuber C., Tecl J. Initial tests of Al-26 fluoride target matrix on MILEA AMS system. *Nucl. Instrum. Methods Phys. Res. B.* 2021, 503, 45–52.
- Miltenberger K. U., Müller A. M., Suter M., Synal H. A., Vockenhuber C. Accelerator mass spectrometry of Al-26 at 6 MV using AlO^- ions and a gas-filled magnet. *Nucl. Instrum. Methods Phys. Res. B.* 2017, 406, 272–277.
- Lachner J., Christl M., Alfimov V., Hajdas I., Kubik P. W., Schulze-König T., Wacker L., Synal H. A. Ca-41, C-14 and Be-10 concentrations in coral sand from the Bikini atoll. *J. Environ. Radioact.* 2014, 129, 68–72.
- Vivo-Vilches C., Lopez-Gutierrez J. M., Garcia-Leon M., Vockenhuber C. Factors related to K-41 interference on Ca-41 AMS measurements. *Nucl. Instrum. Methods Phys. Res. B.* 2019, 438, 193–197.
- Kilius L. R., Beukens R. P., Chang K. H., Lee H. W., Litherland A. E., Elmore D., Ferraro R., Gove H. E. Separation of Al-26 and Mg-26 isobars by negative-ion mass-spectrometry. *Nature* 1979, 282, 488–489.
- Fink D., Meirav O., Paul M., Ernst H., Henning W., Kutschera W., Kaim R., Kaufman A., Magaritz M. Accelerator mass spectrometry at the rehovot pelletron tandem: measurements of abundances of cosmogenic radioisotopes and future prospects. *Nucl. Instrum. Methods Phys. Res. B.* 1984, 5, 123–128.
- Michel R., Bodemann R., Busemann H., Dam R., Gloris M., Lange H., Schnatz-Büttgen M., Herpers U., Schiekel T., Sudbrock F., Holmqvist B., Conde H., Malmberg P., Suter M., Dittrich-Hannen B., Kubik P.-W., Sinal H., Filges D. Cross sections for the production of residual nuclides by low- and medium-energy protons from the target elements C, N, O, Mg, Al, Si, Ca, Ti, V, Mn, Fe, Co, Ni, Cu, Sr, Y, Zr, Nb, Ba and Au. *Nucl. Instrum. Methods Phys. Res. B* 1997, 129, 153–193.
- Veicht M., Kajan I., David J. C., Chen S., Strub E., Mihalcea I., Schumann D. Experiment-based determination of the excitation function for the production of Ti-44 in proton-irradiated vanadium samples. *Phys. Rev. C* 2021, 104, 014615.
- Müller C., Bunka M., Haller S., Köster U., Groehn V., Bernhardt P., van der Meulen N., Türler A., Schibli R. Promising prospects for $^{44}\text{Sc}/^{47}\text{Sc}$ -based theragnostics: application of ^{47}Sc for radionuclide tumor therapy in mice. *J. Nucl. Med.* 2014, 55, 1658–1664.
- Maxeiner S., Synal H. A., Christl M., Suter M., Müller A., Vockenhuber C. Proof-of-principle of a compact 300 kV multi-isotope AMS facility. *Nucl. Instrum. Methods Phys. Res. B.* 2019, 439, 84–89.
- Vockenhuber C., Schulze-König T., Synal H. A., Aeberli I., Zimmermann M. B. Efficient Ca-41 measurements for biomedical applications. *Nucl. Instrum. Methods Phys. Res. B.* 2015, 361, 273–276.
- Mancusi D., Boudard A., Cugnon J., David J. C., Kaitaniemi P., Leray S. Extension of the Liege intranuclear-cascade model to reactions induced by light nuclei. *Phys. Rev. C* 2014, 90, 054602.
- Boudard A., Cugnon J., David J. C., Leray S., Mancusi D. New potentialities of the Liege intranuclear cascade model for reactions induced by nucleons and light charged particles. *Phys. Rev. C* 2013, 87, 014606.
- Kelic A., Ricciardi V., Schmidt K.-H. *ABLA07 – towards a Complete Description of the Decay Channels of a Nuclear System from Spontaneous Fission to Multifragmentation*. Ithaca, NY, USA: Cornell University Library; 2009: p. 4193. arXiv:0906.

20. David J. C. Spallation reactions: a successful interplay between modeling and applications. *Eur. Phys. J. A* 2015, 51, 68.
21. Titarenko Y. E., Shvedov O. V., Batyaev V. F., Karpikhin E. I., Zhivun V. M., Koldobsky A. B., Mulambetov R. D., Kvasova S. V., Sosnin A. N., Mashnik S. G., Prael R. E., Sierk A. J., Gabriel T. A., Saito M., Yasuda H. Cross sections for nuclide production in 1 GeV proton-irradiated ^{208}Pb . *Phys. Rev. C* 2002, 65, 064610.
22. Veicht M., Mihalcea I., Cvjetinovic Đ., Schumann D. Radiochemical separation and purification of non-carrier-added silicon-32. *Radiochim. Acta* 2021, 109, 735–741.

Supplementary Material: The online version of this article offers supplementary material (<https://doi.org/10.1515/ract-2022-0036>).